Applied Catalysis B: Environmental 238 (2018) 1–5

Contents lists available at ScienceDirect

Applied Catalysis B: Environmental

journal homepage: www.elsevier.com/locate/apcatb

New concept for old reaction: Novel WGS catalyst design

Nuria García-Moncada*, Miriam González-Castaño, Svetlana Ivanova, Miguel Ángel Centeno, Francisca Romero-Sarria, José Antonio Odriozola

Departamento de Química Inorgánica e Instituto de Ciencia de Materiales de Sevilla centro mixto CSIC-Universidad de Sevilla, Sevilla, Spain

ARTICLE INFO

Keywords:
WGS
Ionic conductor
Cu catalyst
Au catalyst
Pt catalyst
Water activation
Rate-limiting step

ABSTRACT

The viability of water gas shift catalytic system for mobile application passes through obligatory reactor volume reduction, achieved normally by using less charge of more efficient catalyst. Completely new concept for catalyst design is proposed: a catalytic system including classically reported WGS catalysts of different nature or active phase (Cu, Pt or Au) mechanically mixed with an ionic conductor. The influence of the later on catalyst activity is studied and discussed, more precisely its effect on the rate of the reaction-limiting step and catalysts' efficiency. It is demonstrated with this study, that the presence of an ionic conductor in contact with a WGS catalyst is essential for the water supply (dissociation and transport), thereby potentiating the water activation step, whatever the mechanism and catalyst overall performance.

1. Introduction

One of the oldest catalytic reaction, water gas shift (WGS) reaction possesses the particularity of being slightly exothermic ($CO + H_2O \leftrightarrow CO_2 + H_2$, $\Delta H_R^0 = -41.1$ kJ/mol) and favoured at low temperatures where the kinetics is slow involving low space velocities and large reactor volumes. The necessary reactor obstructs its applicability in mobile devices targeting on board H_2 production. At industrial scale, the WGS reaction is carried out in a series of two adiabatic reactors. In the first one, high temperature water gas shift reaction (HT-WGS) takes place between 350–450 °C on promoted Fe/Cr oxide catalysts reducing the CO content from 10 to 50 wt.% at the reactor inlet to about 3–5 wt.% at the outlet. In the second reactor, Cu based catalysts are applied in the 190–250 °C temperature range, known as Low Temperature Water Gas Shift reaction (LT-WGS) to reduce CO to levels as low as possible [1,2]. Both steps require large reactors and low space velocities (about 3000–4000 h^{-1} for the former and 1000–2000 h^{-1} for the later). The application of those reactors in mobile devices infers 75% occupation of the total possible space if we imagine all necessary units to be applied for H_2 technology, *i.e.* reforming, WGS, PROX reactors and PEM fuel cell. For the later, the CO content of the entering H_2 stream should be obligatory decreased to levels below few ppm [2]. Accordingly, the first step of the overall volume reduction goes through the use of only one WGS reactor at medium temperature. In recent years, noble metal (Pt, Au or Pd) based catalysts are proposed as promising catalysts for medium temperature WGS [1]. Moreover, the use of precious metals could solve the safety problems, like pyrophoricity of the LT-WGS Cu catalyst [3].

For all known catalysts, two general mechanisms are proposed depending on the active phase and reaction conditions. In the redox mechanism the adsorbed CO is firstly oxidized to CO_2 either by dissociated water or by labile oxygen from the support creating an oxygen vacancy. Then, the support is reoxidized by water leading to hydrogen formation [4–6]. On the contrary, the associative mechanism proceeds *via* CO and H_2O co-adsorption on the catalyst surface. The water molecule is dissociated and the surface −OH groups interact with adsorbed CO forming different intermediates (carbonates, carboxylates or formates) [7–10]. The subsequent decomposition of these species leads to CO_2 and H_2 formation. According to the literature and regardless the catalyst (Fe, Cu or noble metal) and mechanism type (redox or associative), the dissociation of water molecules seems to be recognized as the rate-limiting step of the reaction [8,11–15]. Some studies compared the energies of all evolved WGS steps and show that water adsorption and dissociation processes have the highest energetic barriers [8,16,17]. Kinetic studies present also the most positive and highest reaction order for water emphasizing the significant influence of the water concentration on catalyst' reaction rate [17,18]. It is reported that the use of reducible oxides and/or solids presenting oxygen vacancies improve the activity of the employed metals for the shift reaction [1,19]. As an example, González-Castaño et al. [20] studied the influence of Zr and Fe as oxygen vacancies originators to ceria structure in a series of Pt based catalysts for the WGS reaction. Better stability and activity was observed for the bi-doped (Zr and Fe) sample and attributed to the increase of Ce^{3+}/oxygen vacancies active sites number

* Corresponding author.
E-mail address: nuria.garcia@icmse.csic.es (N. García-Moncada).

https://doi.org/10.1016/j.apcatb.2018.06.068
Received 3 April 2018; Received in revised form 23 June 2018; Accepted 26 June 2018
Available online 30 June 2018
0926-3373/

and their participation in H species mobility (OH^- and H^+). The same authors in other study introduced an as called "buffer" layer in structured Pt based catalysts [21]. They observed that an increase of the overall reaction rate is achieved when the buffer layer id added. It is possible then to influence the catalyst activity by an improvement of the rate limiting step allowing higher reaction space velocities and, consequently, reactor volume reduction. To achieve this, an interesting possibility, not really explored, is the development of an ionic conductor, which added to the catalyst, should improve the dissociation and water species diffusion of the water during the reaction.

An ionic conductor, usually created after aliovalent doping of transition or rare earth metal oxides, provide structural oxygen vacancies that facilitates the diffusion of ions, such O^-, O^{2-}, OH^-, H^+ or H_3O^+, issued from oxygen and water dissociation [22]. Considering that mixed aliovalent doped rare-earth oxides generate good ionic conductivity and stable structures in the WGS reaction temperature range [23–26], the main goal of the present work is to find out if their presence improve the activity of existing WGS catalysts. In this way and irrespective to the catalyst' nature, the ionic conductor should provide an improvement of the CO conversion by directly acting on the reaction rate-limiting step.

Hence, the aim of our study is to prove this new concept by preparing a multi component catalytic system consisting of a mixture of different in nature ionic conductors and three different in active phase catalysts (Cu, Au, Pt). Presuming that the three active phases act with differences in their general mechanism but have the same rate-limiting step, the role of the ionic conductor is corroborated.

2. Experimental

2.1. Synthesis of the catalysts

Three different type of catalysts were used: i) $CuO/ZnO/Al_2O_3$ (molar Cu^{2+}/Zn^{2+} and M^{2+}/M^{3+} ratios of 5.6 and 3, respectively), labelled CuZnAl; ii) $Pt/CeO_2/Al_2O_3$ (2 wt.% of Pt over commercial ceria-alumina support), labelled PtCeAl, and iii) $Au/CeO_2/Al_2O_3$ catalyst (2 wt.% of Au over commercial ceria-alumina support), labelled AuCeAl.

The copper based sample (CuZnAl) was obtained from hydrotalcite like precursor after co-precipitation of $Cu(NO_3)_2{\cdot}3H_2O$, $Zn(NO_3){\cdot}6H_2O$ and $Al(NO_3)_3{\cdot}9H_2O$ by 1 M sodium carbonate aqueous solution at controlled pH. After 48 h the resulting solid is filtered, washed, dried at 100 °C overnight and finally calcined at 300 °C for 4 h. Detailed description of the synthesis procedure is proposed in previously reported study [27].

The Pt based catalyst (PtCeAl) was prepared by wet impregnation. The Pt precursor, tetrammine platinum (II) nitrate solution (Johnson Matthey), previously mixed with 1 M acetic acid solution in molar ratio of 1:1.1, was mixed with commercial CeO_2/Al_2O_3 support (Puralox, ceria/alumina mass ratio of 20:80). After, solvent evaporation at reduced pressure in rotary evaporator the resultant solid was dried overnight and calcined at 350 °C for 8 h using a heating rate of 5 °C/min.

Au based catalyst (AuCeAl) was prepared by direct anionic exchange (DAE) method assisted with NH_3 using $2{\cdot}10^{-4}$ M aqueous solution of $HAuCl_4$ (Johnson Matthey) as gold precursor to obtain 2 wt.% of gold on ceria-alumina support (Puralox, ceria/alumina mass ratio of 20:80) as nominal value [28]. The sample was calcined in static air at 350 °C for 4 h.

2.2. Synthesis of the ionic conductors

On the other side, three different ionic conductors were prepared: Eu doped zirconia, (5 mol% of Eu_2O_3), labelled ZrEu; europium molybdate (39 wt.% of Eu), labelled MoEu; and europium niobate, (50 wt.% of Eu), labelled NbEu.

Both ZrEu and MoEu ionic conductors were synthesized by co-precipitation method from metal nitrates or molybdates ($ZrN_2O_7{\cdot}xH_2O$, $Eu(NO_3)_3{\cdot}5H_2O$ and $(NH_4)_6Mo_7O_{24}{\cdot}4H_2O$, respectively) at pH 8 using NH_3 solution for the precipitation. The resulted powder was washed, filtered, dried and calcined at 500 °C for 5 h. The NbEu mixed oxide was prepared by co-precipitation of $Eu(NO_3)_3{\cdot}5H_2O$ and niobium (V) chloride with NH_3 solution at pH 8 during 12 h. The solid was dried and calcined at 800 °C for 1 h.

2.3. Characterization techniques

All solids were characterized by X-ray diffraction (XRD) by using an X'Pert Pro PANalytical instrument. The diffraction patterns were obtained using Cu Kα radiation (40 mA, 45 kV) over a 2θ-range of 10-90° and using a step size of 0.05° and a step time 80 s.

The X-ray fluorescence spectrometry (XRF) was used to determine the active phase content. The analyses were carried out on AXIOS PANalytical spectrometer with Rh source of radiation.

2.4. Catalytic tests

The WGS reaction was carried out in a home-made system including tubular fixed bed reactor working at atmospheric pressure and on-line ABB gas analyser (AO2020) equipped with an IR detector. The catalytic tests were performed in the 180–350 °C temperature range using the as called "model" feed of 4.5% CO, 30% of H_2O and N_2 as balance. Every catalyst was tested separately or in a mixture with one of the ionic conductors. For instance, the bare CuZnAl and the mixtures CuZnAl + ZrEu, CuZnAl + NbEu and CuZnAl + MoEu. These four experiments were also carried out for PtCeAl and AuCeAl catalysts. All experiments were performed at GHSV of 4000 h^{-1} using particles within the 600 and 800 μm range at constant catalytic bed volume. The space velocity was maintained using the same catalyst loading (0.16 g) mixed either with ionic conductor or with inert quartz with the same particle size. Thus, the catalyst charge and bed volume whatever the catalyst were kept constant and only the presence and nature of the ionic conductor was changed, allowing thereby a direct correlation of the WGS activity to the effect of the later. The mixed samples were prepared using 1:2 mass ratio of catalyst: ionic conductor.

3. Results and discussion

The XRD of the catalysts are shown in Fig. 1. CeO_2 fluorite type crystal structure [JCPDS: 00-034-0394] and γ-Al_2O_3 [JCPDS: 01-077-0396] are the only phases detected for the noble metal based catalysts, PtCeAl and AuCeAl. Neither Pt nor Au attributed signals are observed, suggesting good dispersion for the metal loadings neighbouring the targeted value of 2 wt.% (Table 1). For the CuZnAl catalyst the X ray diffractions are dominated by the copper containing phases CuO [JCPDS: 00-045-0937], $CuAl_2O_4$ [JCPDS: 00-033-0448] and malachite phase [JCPDS: 00-041-1390]. No clear Zn containing phases contribution is observed although the nominal Cu/Zn ratio obtained (Table 1).

As for the ionic conductors cubic solid solution [$Eu_xZr_{1-x}O_\delta$ JCPDS: 01-078-1303], tetragonal phase [$EuMoO_4$ JCPDS: 00-022-1097] and monoclinic phase [$EuNbO_4$ JCPDS: 00-022-1099] of mixed oxides are formed with the introduction of the europium (Fig. 2). Doping the niobates and molybdates with rare-earth metals, like Eu, has been reported to create well-organized oxygen vacancies rich mixed oxides, generating intrinsic ionic conductivity [23,26,29–33]. On the other hand, doped zirconia is often reported to present a pure ionic conductivity increased in presence of water by the as called Grotthuss mechanism allowing extra proton conductivity at lower temperatures. In this process, a translational dynamics of a bigger molecule named "vehicle" assists the proton diffusion [34]. Concretely, in the Grotthuss mechanism, the H_2O molecules act as vehicle species for the proton mobility by H_3O^+ formation. This additional reorganization of the

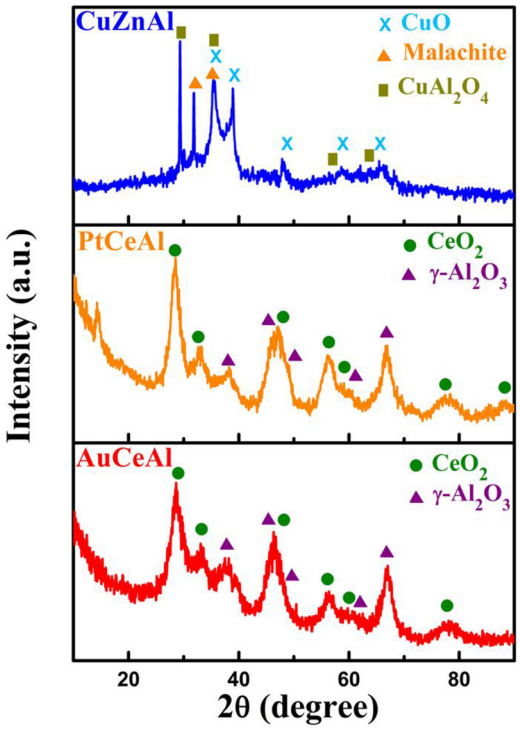

Fig. 1. XRD of the synthesized catalysts.

Table 1
Chemical composition of the synthesized catalysts by XRF (wt.%).

CuZnAl	PtCeAl	AuCeAl
63.2 CuO	1.8 Pt	2.3 Au
10.7 ZnO	18.8 CeO_2	20.6 CeO_2
26.1 Al_2O_3	79.4 Al_2O_3	77.1 Al_2O_3

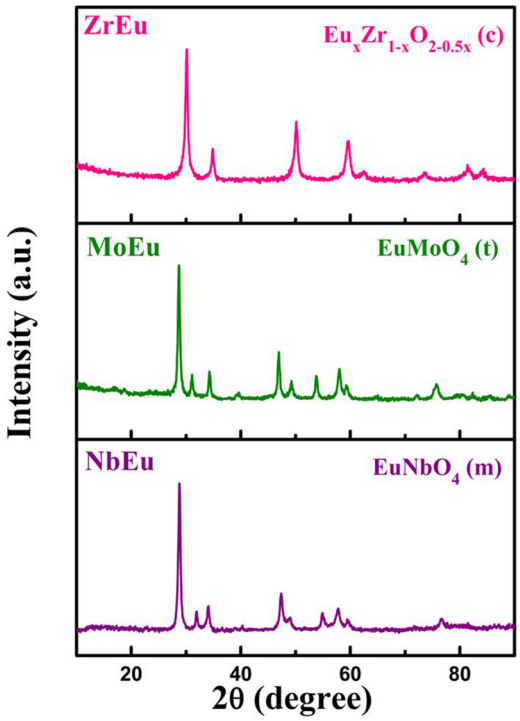

Fig. 2. XRD of the synthesized mixed oxides.

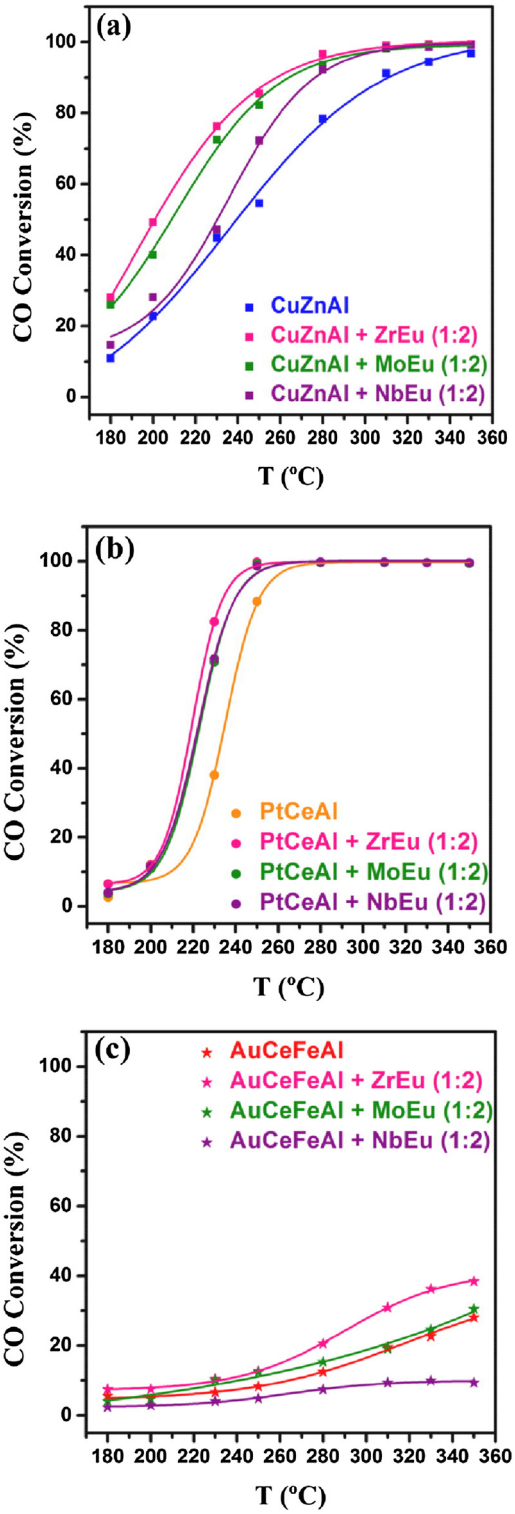

Fig. 3. Catalytic tests for WGS reaction at 4000 h^{-1} using a model feed (4.5% CO and 30% H_2O in N_2 flow) over 0.16 g of (a) CuZnAl catalyst, (b) PtCeAl catalyst and (c) AuCeAl catalyst. Bare catalyst' activity compared with their physical mixtures with different ionic conductors.

proton environment, comprising H_2O molecules reorientation, creates an uninterrupted trajectory for the proton migration [35].

The comparative studies of the samples with or without ionic conductor for the WGS reaction in the same model conditions of feeding, particle size and space velocity are shown in Figs. 3 and 4. In order to roughly compare the catalysts' activities with different nature and

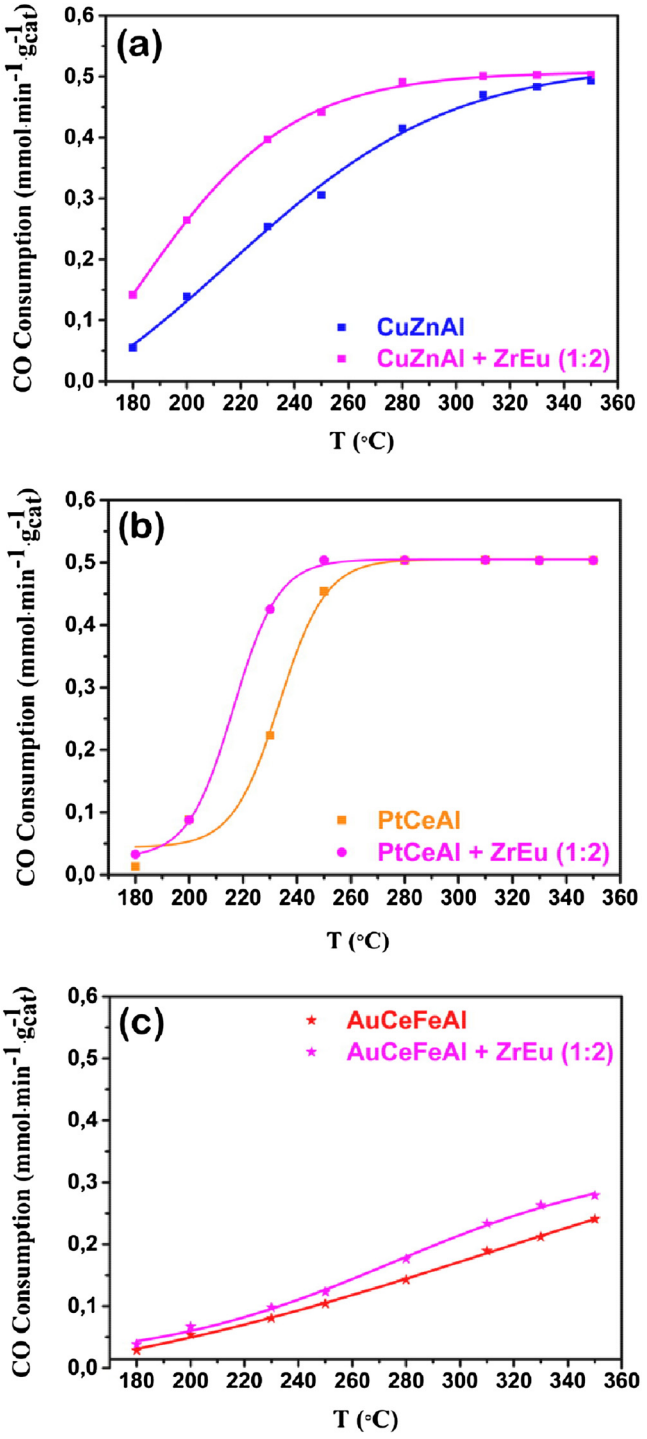

Fig. 4. Calculated normalized CO consumption rate per weight of catalyst in WGS reaction at 4000 h^{-1} using a model feed (4.5% CO and 30% H_2O in N_2 flow) on (a) CuZnAl catalyst, (b) PtCeAl catalyst and (c) AuCeAl catalyst. Bare catalyst' activity compared with their physical mixtures with ZrEu ionic conductor.

mechanism (Cu, Pt or Au based catalysts), normalized CO consumption rates have been calculated for the bare catalysts and for their promoted homologue (Fig. 4): The ZrEu ionic conductor was employed as it provides the highest effect in all cases. The catalyst' activity varies in order CuZnAl > PtCeAl > AuCeAl at low temperature. The Cu based catalyst is the most active at low temperatures, but the activity of the Pt based catalyst achieves rapidly at 230 °C the same activity ~ 0.24 mmol of CO consumed per min and per weight of catalyst. It is also noticeable the PtCeAl catalyst is the first to achieve maximum CO conversion (Fig. 3). The activities of the catalysts are in agreement with other studies for similar samples found elsewhere [36–39]. Hence, this activity trend is expected taking into account that copper sample starts working at lower temperatures (10% of CO conversion at 180 °C) and, on the other hand, the gold and Pt based catalysts show better performances at higher temperatures (from around 240 °C). The gold based catalyst shows lower activity in comparison to its Pt homologue for a similar metal loading, caused probably by differences in the metal state, either bigger gold particles and therefore lower specific activity or insufficient synergy between the support and metal sites. It was reported that the different catalytic behaviour of Pt and Au is caused by the impossibility of gold to activate dissociatively the water molecules, being this the reason of lower WGS activity for Au at similar Pt charge and dispersion [40]. Taking into account the aim of this study, to find a universal WGS activity promoter, the intrinsic activity of the samples is not the most important item. In fact, for that goal, there should be some catalytic activity and if possible, differences in the considered WGS mechanism and in the activity temperature range.

When the ionic conductor is added to the catalyst bed, no matter the nature of catalyst or that of ionic conductor itself, the catalysts activity, in terms of CO conversion, increases. The ionic conductor behaviour is strictly related to catalyst' proper reaction mechanism. Meanwhile benefits Cu based catalyst in the 180–250 °C temperature range, makes the same for Pt in the 230–280 °C range. Even for the Au based catalyst, the effect of the ionic conductor is exhibited rapidly when the catalyst starts to work (around 230–250 °C). This observation confirms the statement that the ionic conductor should potentiate only the water activation step, *i.e.* dissociation species and diffusion. The universality of the concept is approved by the fact that the ionic conductor presence only helps the catalyst when start working, no matter temperature range or mechanism, being the later related only to the catalyst' nature. No WGS activity of the ionic conductors or quartz diluent was observed.

It is essential to be aware that a possible positive effect could arise from the dilution and/or thermic effects after the addition of the ionic conductor. Considering that the catalysts particles are composed by both, catalyst and conductor, the former is already diluted improving the internal diffusion and enhancing the thermal dissipation during the reaction. However, for AuCeAl catalyst, presenting the lowest conversion, a low thermal effect is expected. The similar curve shape in presence or absence of ionic conductor and the increased WGS activity indicates that this beneficial effect in these conditions is mainly due to the improvement of the water activation step. The calculated Thiele modulus in these conditions results below 1 (with or without the ionic conductor), indicating that there are not internal diffusional problems.

It is also noticeable in Fig. 3 that although the same trend for all conductors is observed, the ZrEu formulation seems to provide the highest effect on the catalyst performance. Within the series with the same catalyst, the variation in the CO conversion will depend on the ionic conductor nature, as it was already demonstrated [41]. The ionic conductor structure, its chemical and mechanical stability, and all features related to its conductivity: oxygen vacancies concentration, mobility, organization, accessibility and stability [25,42–44] determine its influence on catalysts' WGS behaviour. Within the group of three conductors, europium substituted niobates and molybdates possess a strictly stoichiometric formulation while the ZrEu mixed oxide forms a solid solution in a high range of oxygen sub-stoichiometric structures (Eq. 1). This property provides to the later higher ionic conductivity through easier oxygen vacancies mobility according to a p-type semiconductor [22].

$$x\,Eu_2O_3(ZrO_2) \rightarrow 2x\,Eu'_{Zr} + 3xO_O^x + xV_O^{2\cdot} \quad (1)$$

More specifically, the promoter effect exercised on catalyst by each conductor is directly related to the number of additional sites (vacancies) for water activation.

4. Conclusions

The successful development of a multicomponent catalytic system based on a physical mixture of an ionic conductor and a WGS catalyst is confirmed by the important beneficial effect observed on catalyst' activity. No matter the ionic conductor catalyst' nature, the presence of the former potentiates the water activation step independently of catalyst' reaction mechanism. The real ionic conductor effect appears when the catalyst starts to work, only helping its activity by providing more dissociated water species and proton conductivity by Grotthuss mechanism.

No matter the catalyst nature, the same trend of influence ZrEu > MoEu > NbEu is observed, indicating that the ZrEu ionic conductor is the most appropriated one for the WGS reaction in these operation conditions, probably due to the higher oxygen vacancies concentration allowed by its sub-stoichiometric structure.

Acknowledgement

We acknowledge financial support for this work from the Spanish Ministerio de Economía y Competitividad (MINECO) (ENE2015-66975-C3-2-R).

References

[1] C. Ratnasamy, J.P. Wagner, Water gas shift catalysis, Catal. Rev.: Sci. Eng. 51 (2009) 325–440.
[2] R.J. Farrauto, Y. Liu, W. Ruettinger, O. Ilinich, L. Shore, T. Giroux, Precious metal catalysts supported on ceramic and metal monolithic structures for the hydrogen economy, Catal. Rev.: Sci. Eng. 49 (2007) 141–196.
[3] R. Kam, J. Scott, R. Amal, C. Selomulya, Pyrophoricity and stability of copper and platinum based water-gas shift catalysts during oxidative shut-down/start-up operation, Chem. Eng. Sci. 65 (2010) 6461–6470.
[4] S. Hilaire, X. Wang, T. Luo, R.J. Gorte, J. Wagner, A comparative study of water-gas-shift reaction over ceria supported metallic catalysts, Appl. Catal. A: Gen. 215 (2001) 271–278.
[5] R.J. Gorte, S. Zhao, Studies of the water-gas-shift reaction with ceria-supported precious metals, Catal. Today 104 (2005) 18–24.
[6] C.M. Kalamaras, P. Panagiotopoulou, D.I. Kondarides, A.M. Efstathiou, Kinetic and mechanistic studies of the water-gas shift reaction on Pt/TiO_2 catalyst, J. Catal. 264 (2009) 117–129.
[7] R.J. Madon, D. Braden, S. Kandoi, P. Nagel, M. Mavrikakis, J.A. Dumesic, Microkinetic analysis and mechanism of the water gas shift reaction over copper catalysts, J. Catal. 281 (2011) 1–11.
[8] A.A. Gokhale, J.A. Dumesic, M. Mavrikakis, On the mechanism of low-temperature water gas shift reaction on copper, J. Am. Chem. Soc. 130 (2008) 1402–1414.
[9] G. Jacobs, U.M. Graham, E. Chenu, P.M. Patterson, A. Dozier, B.H. Davis, Low-temperature water-gas shift: impact of Pt promoter loading on the partial reduction of ceria and consequences for catalyst design, J. Catal. 229 (2005) 499–512.
[10] G. Germani, Y. Schuurman, Water-Gas Shift Reaction Kinetics Over μ-Structured Pt/CeO_2/Al_2O_3 Catalysts Vol. 52 American Institute of Chemical Engineers, 2006, pp. 1806–1813.
[11] T. Ramírez Reina, S. Ivanova, V. Idakiev, J.J. Delgado, I. Ivanov, T. Tabakova, M.A. Centeno, J.A. Odriozola, Impact of Ce–Fe synergism on the catalytic behaviour of Au/CeO_2-FeO_x/Al_2O_3 for pure H_2 production, Catal. Sci. Technol. 3 (2013) 779–787.
[12] G. Wang, L. Jiang, Y. Zhou, Z. Cai, Y. Pan, X. Zhao, Y. Li, Y. Sun, B. Zhong, X. Pang, W. Huang, K. Xie, Investigation of the kinetic properties for the forward and reverse WGS reaction by energetic analysis, J. Mol. Struct.: THEOCHEM 634 (2003) 23–30.
[13] J.A. Rodriguez, P. Liu, J. Hrbek, J. Evans, M. Pérez, Water gas shift reaction on Cu and Au nanoparticles supported on CeO_2(111) and ZnO(0001): intrinsic activity and importance of support interactions, Angew. Chem. Int. Ed. 46 (2007) 1329–1332.
[14] L.C. Grabow, A.A. Gokhale, S.T. Evans, J.A. Dumesic, M. Mavrikakis, Mechanism of the water gas shift reaction on Pt: first principles, experiments, and microkinetic modeling, J. Phys. Chem. C 112 (2008) 4608–4617.
[15] C.V. Ovesen, B.S. Clausen, B.S. Hammershoi, G. Steffensen, T. Askgaard, I. Chorkendorff, J.K. Norskov, P.B. Rasmussen, P. Stoltze, P. Taylor, A microkinetic analysis of the water-gas shift reaction under industrial conditions, J. Catal. 158 (1996) 170–180.
[16] J.P. Clay, J.P. Greeley, F.H. Ribeiro, W.N. Delgass, W.F. Schneider, DFT comparison of intrinsic WGS kinetics over Pd and Pt, J. Catal. 320 (2014) 106–117.
[17] A.A. Phatak, N. Koryabkina, S. Rai, J.L. Ratts, W. Ruettinger, R.J. Farrauto, G.E. Blau, W.N. Delgass, F.H. Ribeiro, Kinetics of the water-gas shift reaction on Pt catalysts supported on alumina and ceria, Catal. Today 123 (2007) 224–234.
[18] G.N. Vajani, S.L. Ng, C.R.F. Lund, Rate expression for water-gas shift over a gold/ferrochrome catalyst, Ind. Eng. Chem. Res. 50 (2011) 10493–10499.
[19] X. Wang, J.A. Rodriguez, J.C. Hanson, M. Pérez, J. Evans, In situ time-resolved characterization of Au–CeO_2 and AuO_x–CeO_2 catalysts during the water-gas shift reaction: presence of Au and O vacancies in the active phase, J. Chem. Phys. 123 (2005) 221101–1–221101–5.
[20] M. González-Castaño, S. Ivanova, T. Ioannides, M.A. Centeno, J.A. Odriozola, Deep insight into Zr/Fe combination for successful Pt/CeO_2/Al_2O_3 WGS catalyst doping, Catal. Sci. Technol. 7 (2017) 1556–1564.
[21] M. González-Castaño, S. Ivanova, O.H. Laguna, L.M. Martínez, M.A. Centeno, J.A. Odriozola, Structuring Pt/CeO_2/Al_2O_3 WGS catalyst: introduction of buffer layer, Appl. Catal. B: Environ. 200 (2017) 420–427.
[22] R.J.D. Tilley, Defects in Solids, WILEY, New Jersey, 2008.
[23] G. Adachi, N. Imanaka, S. Tamura, Ionic conducting lanthanide oxides, Chem. Rev. 102 (2002) 2405–2429.
[24] V. Besikiotis, C.S. Knee, I. Ahmed, R. Haugsrud, T. Norby, Crystal structure, hydration and ionic conductivity of the inherently oxygen-deficient $La_2Ce_2O_7$, Solid State Ionics 228 (2012) 1–7.
[25] V. Besikiotis, S. Ricote, M.H. Jensen, T. Norby, R. Haugsrud, Conductivity and hydration trends in disordered fluorite and pyrochlore oxides: a study on lanthanum cerate-zirconate based compounds, Solid State Ionics 229 (2012) 26–32.
[26] X.-L. Xia, Z.-G. Liu, J.-H. Ouyang, Y. Zheng, Preparation, structural characterization, and enhanced electrical conductivity of pyrochlore-type $(Sm_{1-x}Eu_x)_2Zr_2O_7$ ceramics, Fuel Cells 12 (4) (2012) 624–632.
[27] J.L. Santos, T.R. Reina, S. Ivanova, M.A. Centeno, J.A. Odriozola, Gold promoted Cu/ZnO/Al_2O_3 catalysts prepared from hydrotalcite precursors: advanced materials for the WGS reaction, Appl. Catal. B: Environ. 201 (2017) 310–317.
[28] S. Ivanova, C. Petit, V. Pitchon, A new preparation method for the formation of gold nanoparticles on an oxide support, Appl. Catal. A: Gen. 267 (2004) 191–201.
[29] R. Haugsrud, T. Norby, High-temperature proton conductivity in acceptor-doped $LaNbO_4$, Solid State Ionics 177 (2006) 1129–1135.
[30] J.E. Vega-Castillo, U.K. Ravella, G. Corbel, P. Lacorre, A. Caneiro, Thermodynamic stability, structural and electrical characterization of mixed ionic and electronic conductor $La_2Mo_2O_{8.96}$, Dalton Trans. 41 (2012) 7266–7271.
[31] V. Morozov, A. Arakcheeva, B. Redkin, V. Sinitsyn, S. Khasanov, E. Kudrenko, M. Raskina, O. Lebedev, G. Van Tendeloo, $Na_{2/7}Gd_{4/7}MoO_4$: a modulated scheelite-type structure and conductivity properties, Inorg. Chem. 51 (2012) 5313–5324.
[32] D. Marrero-López, P. Núñez, M. Abril, V. Lavín, U.R. Rodríguez-Mendoza, V.D. Rodríguez, Synthesis, electrical properties, and optical characterization of Eu^{3+}-doped $La_2Mo_2O_9$ nanocrystalline phosphors, J. Non-Crystalline Solids 345–346 (2004) 377–381.
[33] M. Nyman, M.A. Rodriguez, T.M. Alam, T.M. Anderson, A. Ambrosini, Aqueous synthesis and structural comparison of rare earth niobates and tantalates: $(La,K,\square)_2Nb_2O_{7-x}(OH)_2$ and $Ln_2Ta_2O_7(OH)_2$ (□ = vacancy; Ln = La − Sm), Chem. Mater. 21 (2009) 2201–2208.
[34] K.-D. Kreuer, A. Rabenau, W. Weppner, Vehicle mechanism, a new model for the interpretation of the conductivity of fast proton conductors, Angew. Chem. Int. Ed. Engl. 21 (1982) 208–209.
[35] C.J.T. van Grotthuss, Sur la décomposition de l'eau et des corps qu'elle tient en dissolution à l'aide de l'électricité galvanique, Ann. Chim. 58 (1806) 54–73.
[36] M. Gonzalez Castaño, T.R. Reina, S. Ivanova, M.A. Centeno, J.A. Odriozola, Pt vs. Au in water-gas shift reaction, J. Catal. 314 (2014) 1–9.
[37] T.R. Reina, S. Ivanova, M.A. Centeno, J.A. Odriozola, Boosting the activity of a Au/CeO_2/Al_2O_3 catalyst for the WGS reaction, Catal. Today 253 (2015) 149–154.
[38] D. Li, S. Xu, Y. Cai, C. Chen, Y. Zhan, L. Jiang, Characterization and catalytic performance of Cu/ZnO/Al_2O_3 water- gas shift catalysts derived from Cu-Zn-Al layered double hydroxides, Ind. Eng. Chem. Res. 56 (2017) 3175–3183.
[39] D. Andreeva, I. Ivanov, L. Ilieva, J.W. Sobczak, G. Avdeev, K. Petrov, Gold based catalysts on ceria and ceria-alumina for WGS reaction (WGS Gold catalysts), Top. Catal. 44 (2007) 173–182.
[40] M. González-Castaño, T.R. Reina, S. Ivanova, L.M. Martínez Tejada, M.A. Centeno, J.A. Odriozola, O_2-assisted water gas shift reaction over structured Au and Pt catalysts, Appl. Catal. B: Environ. 185 (2016) 337–343.
[41] N. García-Moncada, L.F. Bobadilla, R. Poyato, C. López-Cartes, F. Romero-Sarria, M.Á. Centeno, J.A. Odriozola, A direct *in situ* observation of water-enhanced proton conductivity of Eu-doped ZrO_2: effect on WGS reaction, Appl. Catal. B: Environ. 231 (2018) 343–356.
[42] L. Malavasi, C.A.J. Fisher, M.S. Islam, Oxide-ion and proton conducting electrolyte materials for clean energy applications: structural and mechanistic features, Chem. Soc. Rev. 39 (2010) 4370–4387.
[43] C.-T. Chen, S. Sen, S. Kim, Effective concentration of Mobile oxygen-vacancies in heavily doped cubic zirconia: results from combined electrochemical impedance and NMR spectroscopies, Chem. Mater. 24 (2012) 3604–3609.
[44] K.D. Kreuer, Aspects of the formation and mobility of protonic charge carriers and the stability of perovskite-type oxides, Solid State Ionics 125 (1999) 285–302.